Drug Development and Industrial Pharmacy, 34:559–568, 2008

ISSN: 0363-9045 print / 1520-5762 online
DOI: 10.1080/03639040701657552

informa
healthcare

The Spray Drying of Unfractionated Heparin: Optimization of the Operating Parameters

Jagdeep Shur, Thomas G. Nevell, Janis K. Shute, and James R. Smith

School of Pharmacy and Biomedical Sciences, Institute of Biomedical and Biomolecular Science, University of Portsmouth, St. Michael's Building, White Swan Road, Portsmouth, UK

Unfractionated heparin is an anti-inflammatory mucoactive agent, with the potential to treat the inflamed and mucus-obstructed airways in patients with cystic fibrosis. In this study, unfractionated heparin has been spray-dried to produce spherical micronized particles in the size range 1–5 μm, which is suitable for delivery by dry-powder inhalation. Spray drying parameters have been optimized using a 2^4 factorial experimental design. The feed concentration and atomization spray flow rate have the greatest effects on recovery (typically 60%) and particle size.

Keywords spray drying; factorial experimental design; unfractionated heparin; pulmonary drug delivery; cystic fibrosis; dry-powder inhaler

INTRODUCTION

Cystic fibrosis (CF) is the most common lethal autosomal-recessive hereditary disorder of the Western world, affecting 0.025–0.05% of live births in Caucasian populations and with lower incidences in other ethnic groups (Davis, Drumm, & Konstan, 1996). The disease is caused by the inheritance of two mutations in the gene that encodes the CF transmembrane conductance regulator (CFTR). This protein forms chloride ion channels on the apical membranes of epithelial cells (Linsdell, 2006; Riordan, 2005) and hence CF is a multiorgan disease. Morbidity and mortality, however, are associated mainly with lung disease, which is characterized by the accumulation of dehydrated secretions that obstruct initially the small airways (Blouquit et al., 2006) and subsequently the large airways (Boucher, 2004), inviting infection, inflammation, and the progressive destruction of the tissue (Davis et al., 1996).

The retained secretion has an abnormally high viscoelasticity, which in part may be associated with an atypical mucin network (Perez-Vilar & Boucher, 2004) but is due largely to high concentrations of DNA and F-actin, the products of inflammatory cell necrosis (Lethem, James, Marriott, & Burke, 1990; Vasconcellos et al., 1993). Together with native lung mucin polymers, these pathologic components form a tangled network, held together by electrostatic forces, hydrogen bonds, and van der Waals forces (King & Rubin, 2002), that hinders the diffusion of macromolecular drugs and colloidal drug carriers (Sanders, De Smedt, & Demeester, 2000). Thus the mucus both obstructs the airways, decreasing airflow and inviting infection, and acts as a barrier to the delivery of inhaled drugs, including fluticasone (Balfour-Lynn, Klein, & Dinwiddie, 1997), and the vectors used to deliver gene therapy in CF patients (Kitson et al., 1999). Furthermore, it has been shown recently that currently available mucolytics are unlikely to be effective in improving delivery of gene therapy vectors to the airway epithelium, indicating a need for novel agents (Broughton-Head, Smith, Shur, & Shute, 2006).

Mucus clearance through coughing or the mucociliary escalator may be facilitated by disruption of the cross-linking and other interactions between entangled components within the gel. King and Rubin (2002) have suggested that charged oligosaccharides such as dextran sulfate and low-molecular-weight heparin (LMWH) would interfere with hydrogen bonding and ion bonding in mucus gels, and have shown that LMWH improves mucociliary clearance of dog mucus. Unfractionated heparin (UFH; Figure 1) has a number of anti-inflammatory properties (Tyrrell, Horne, Holme, Preuss, & Page, 1999), and we have demonstrated that UFH is mucoactive, significantly reducing the elasticity and yield stress of CF sputum (Broughton-Head, Carroll, & Shute, 2005). Thus, inhaled UFH has potential as an anti-inflammatory and mucolytic therapy for the treatment of CF lung disease.

Clinical trials have established that inhaled nebulized UFH at 25,000 units daily for 7 days (Ledson, Gallagher, Hart, & Walshaw, 2001) and 50,000 units twice a day for 14 days (Serisier et al., 2006) is safe in patients with CF, indicating its therapeutic potential for this condition. However, it was concluded that higher doses may be required to demonstrate significant effects on sputum clearance (Serisier et al., 2006). Studies of the deposition and clearance of inhaled nebulized heparin in the normal healthy lung (Bendstrup, Chambers, Jensen, &

Address correspondence to James R. Smith, School of Pharmacy and Biomedical Sciences, Institute of Biomedical and Biomolecular Science, University of Portsmouth, St. Michael's Building, White Swan Road, Portsmouth, P01 2DT, UK. E-mail: james.smith@port.ac.uk

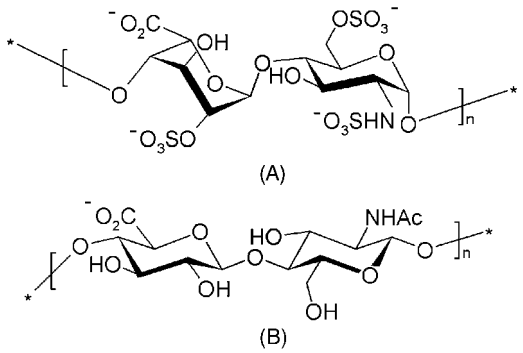

FIGURE 1. Representative repeat unit structures in heparin: (A) the tetra-anionic disaccharide of α-L-idopyranosiduronic acid (1→4) linked to *N*-sulfo-D-glucosamine [α-L-IdoA2S(1–4)α-D-GlcNS6S] (most highly charged structure), and (B) a disaccharide of β-D-glucopyranosiduronic acid (1→4) linked to *N*-acetyl-D-glucosamine [β-D-GlcA(1–4)α-D-GlcNAc] (lowest charge repeating sequence. Adapted from .Fernández, Hattan, & Kerns, 2006.

Newhouse, 1999a; Bendstrup, Gram, & Jensen, 2002; Bendstrup, Newhouse, Pedersen, & Jensen, 1999b) have also shown that inhaled heparin is safe, with doses up to 400,000 units being without significant effect on systemic coagulation parameters. However, as with most nebulized drugs, only 8–12% of the nebulizer charge reaches the lower respiratory tract (LRT) and delivery is prolonged; for example, the highest LRT dose of 32,000 units was nebulized over 60 min.

Nebulizers are used to deliver a number of drugs to the CF airway (e.g., Pulmozyme® and Tobi®) one of the advantages being delivery of high total mass, but there are a number of disadvantages (Geller, 2005; Le Brun, de Boer, Heijerman, & Frijlink, 2000). Because the use of nebulizers is time-consuming, patient compliance is low, resulting in undertreatment of the condition. They also require a source of compressed air, are generally less portable than other devices, and require equipment maintenance and cleaning for infection control.

Dry-powder inhalers (DPIs) are efficient systems for pulmonary drug delivery (Frijlink & de Boer, 2004), with several advantages over nebulizers (Geller, 2005). These delivery systems are portable, propellant-free systems that require less coordination from the patient, are easier to use, and are quicker to deliver a therapeutic dosage to the lung. A powder formulation for inhalation has to meet criteria for dose reproducibility, physicochemical stability, and fine-particle deposition in the respiratory tract. Particle size distribution is important for DPIs, targeting specific regions of the lung, with particles of approximately 5 and 2–3 μm being deposited, respectively, in the central and peripheral airways (Heyder, 2004). Because much of the inflammation and mucus formation occur in the peripheral airways of the CF lung (Blouquit et al., 2006), the particle sizes of dry UFH particles are 2–3 μm, with increased deposition in congested airways (Martonen, Katz, & Cress, 1995). UFH microparticles in this size range have the potential for use in DPI systems, which would offer many advantages over nebulizers.

In producing dry powders with a required particle size-range to ensure deposition at the site of action (Byron & Patton, 1994), high-energy dispersive processes (e.g., mechanical milling) are too destructive to be used for UFH, which, extracted from biological sources (porcine intestine mucin), is a lyophilized and hygroscopic material. Furthermore, the large complex polymeric structure of UFH (Figure 1) renders the materials difficult to crystallize. However, because UFH is highly soluble in water, spray drying is an appropriate method for producing potentially inhalable dry powders. This process, which has been previously used to produce micron- and submicron-sized particles of active agents (Broadhead, Rouan, & Rhodes, 1992), involves a single continuous process that converts liquid feed into dried particulate form. This process offers advantages over other drying methods, including control of the size, morphology, and density of particles (Broadhead et al., 1992; Masters, 1985). A key advantage of spray drying is that it allows the selection and control of operational parameters, so as to produce materials with varied physicochemical properties. The most important operating parameters are inlet temperature (the temperature at which feed solution enters the dryer), aspirator level (rate at which drying air is drawn into the system), pump speed (rate at which feed solution enters the system), spray flow rate (atomization energy), and feed solution concentration.

In pharmaceutical processing, the effects of process parameters on the resulting physicochemical properties of materials are rarely known from the outset. An experimental design protocol is a useful means of establishing the effects of process methodology on product properties and for subsequent optimization (Lewis, Mathieu, & Phan-Tan-Luu, 1999). In the widely used 2^n design, each of the n process variables is set at two levels. Such designs establish the most significant effects on product characteristics both of individual parameters and interacting factors.

With the aim of optimizing the spray-drying conditions required for producing high yields of UFH particles in the required size range, we have used a 2^4 factorial design (Coleman & Montgomery, 1993; Haaland, 1989; Montgomery, 1997) to investigate the effects of feed pump speed, spray flow rate, inlet air temperature, and feed concentration on the product and performance characteristics. The products have been characterized by spectroscopic and physicochemical techniques.

MATERIALS AND METHODS

Spray Drying

UFH solutions (*D*, Table 1) were prepared by adding double-distilled water to sodium UFH (porcine intestinal mucosa; Calbiochem, Nottingham, UK). The small-scale spray dryer (model B-290, Büchi, Labortechnik AG, Flawil, Switzerland) incorporated a standard cyclone and was fitted with a coaxial two-fluid atomizer (compressed air) with an orifice of 0.7 mm (for dilute aqueous solutions). The nozzle was also equipped with automated cooling and cleaning systems.

TABLE 1
Factors and Levels for the Factorial Experiment

Factor		Low Level	High Level
Feed pump speed (cm^3/min)	*A*	5	8
Spray flow rate (dm^3/h)	*B*	500	700
Inlet air temperature (°C)	*C*	160	180
Feed concentration (% wt/vol)	*D*	2	5

The relative humidity (RH) of the drying air before heating was 20%, and both the inlet and outlet air temperatures were monitored. Each process yield was obtained by weighing the product from a metered volume of solution.

To investigate the effects on yield and product characteristics of varying the spray-drying conditions, two levels "low" and "high" values, were used (Table 1) for each of the operating parameters: *A*, feed pump rate; *B*, spray flow rate; *C*, inlet temperature; and *D*, feed concentration. A full factorial experiment of 16 runs was carried out using combinations according to a factorial design matrix with a randomized running order (Taguchi, 1987).

Particle Size, Shape, and Properties

Dry powders, dispersed at a pressure of 2.0 bar, were sized using a laser diffractometer (RODOS feeder, HELOS laser diffractometer, Sympatec GmbH; minimum measurable size, 0.1 μm). Analysis of the particle size distribution was performed using the WINDOX 4.0 software, and 10, 50, and 90% undersize particle size values (X_{10}, X_{50} and X_{90}, respectively, means of three determinations) were obtained.

The true densities of both unprocessed and spray-dried UFHs were determined using helium gas pycnometry (×3; Accupyc 1330 Gas Pycnometer, Micromeritics Instrument Corp., Norcross, GA, USA). Changes were measured under the conditions of helium pressure in a calibrated volume (25°C), containing a weighed amount of dried powder sample.

For scanning electron microscopy (SEM; Joel JSM-35, MA, USA), samples were dusted onto self-adhesive carbon discs and sputter-coated with gold. X-ray powder diffraction (XRPD) patterns were obtained using a Phillips PW1820 diffractometer (Cu K_α, 45 kV, 30 mA; 2 θ: 2–50°, step size 0.02°, ambient conditions). Infrared (IR) spectra (400–4,000 cm^{-1}, resolution 4 cm^{-1}) of samples incorporated into potassium bromide discs were obtained.

Thermal Analysis

Hyper differential scanning calorimetry (HDSC, range: –15 to +200°C, heating rate 10–500 K/min, under helium 30 cm^3/min) was carried out using a Diamond DSC (Perkin-Elmer, Shelton, CT, USA; calibrated with melting onsets: indium 156.0°C and zinc 419.5°C, and a glass transition: amorphous lactose 110°C), with samples (×3; 1–3 mg) in sealed pans. For enhanced baseline reproducibility, two reference pans were used.

The mass losses on heating of unprocessed and spray-dried UFHs were determined by thermogravimetric analysis (TGA 2950, TA Instruments, New Castle, DE, USA) with samples (×3; ~5 mg) under dry nitrogen (50 cm^3/min).

Sorption of Water Vapor

Dynamic vapor sorption (DVS) of water was measured using a microbalance (Surface Measurement Systems, London, UK), enclosed in a humidity-controlled environment at 25°C. RH (0–95%) was determined by selecting the flow rates (50–200 cm^3/min), respectively, of dry and water-saturated nitrogen. Sample masses were monitored continuously during and following imposed changes in RH.

RESULTS AND DISCUSSION

Characterization of Materials

Physical Characteristics of UFH Before and After Spray Drying

The XRPD patterns for spray-dried UFH showed no distinct reflections and were typical of those for amorphous materials; they were indistinguishable from those for the feed material. The IR spectra of the two materials were also very similar, with intense broad bands (~3,450 cm^{-1}), indicating that considerable amounts of water were associated with both forms. The spray-dried UFH, however, was significantly less dense (unprocessed UFH: 1.914 ± 0.001 g/cm^3; spray-dried UFH: 1.896 ± 0.001 g/cm^3). TGA showed losses of 10.9 ± 0.2% (wt/wt) for unprocessed UFH and 11.5 ± 0.3% (wt/wt) for spray-dried UFH (Figure 2) over 20–240°C, but the total losses

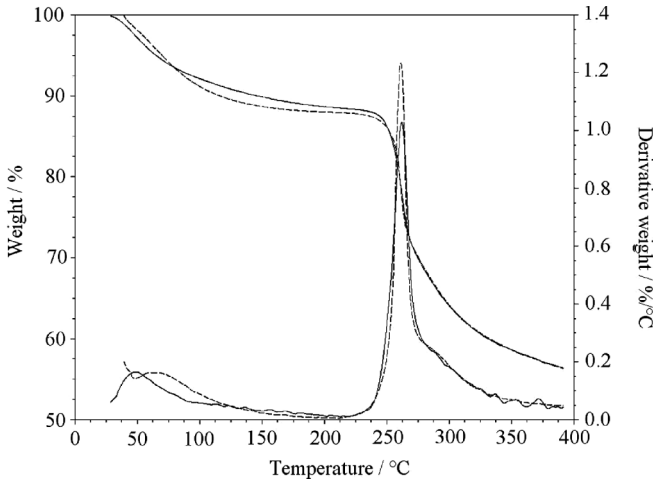

FIGURE 2. Thermogravimetry (20–400°C) of unprocessed unfractionated heparin (UFH) (continuous lines) and spray-dried UFH (broken lines); samples ~5 mg in open pans under N_2, heating rate 5 K/min.

of mass corresponded (±0.1%) at 260°C and higher temperatures. These results indicate that the total amount of water associated with the two forms was similar but that a small proportion (~0.6% of the sample mass) was more strongly bound in the unprocessed material and was responsible for the higher density.

Representative SEM images (Figure 3) show unprocessed UFH to consist of irregular plates with a wide range of sizes (by inspection, ~50–800 μm) typical of lyophilized powders, whereas spray drying, under all process conditions used, produced smooth spherical particles (~0.1–5 μm, in small samples), with some showing surface dimples characteristic of the spray-drying process. Some individual particles formed loose agglomerates (5–20 μm), possibly due to areas of contact (and hence also inter-particulate attraction forces) being increased by the slight deformation of touching particles. Alternatively, surface moisture forming a thin layer between touching particles would have given rise to attractive capillary forces.

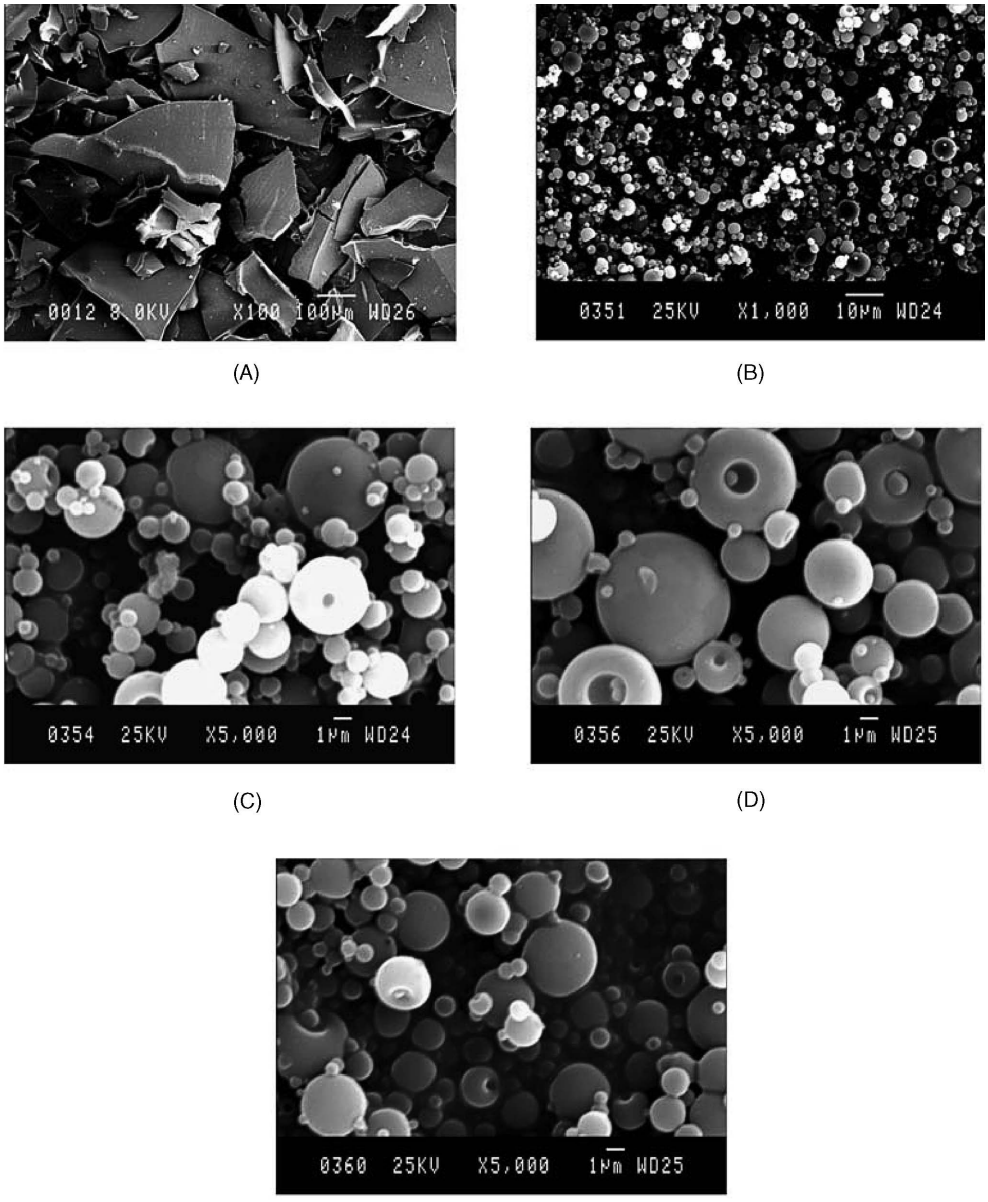

FIGURE 3. SEM images of (A) unprocessed unfractionated heparin (UFH) (low resolution) and (B) spray-dried UFH (low resolution). Images showing the effects of spray flow rate B and feed concentration D on particle shape and diameter (inlet temperature 160°C, pump speed 8 cm^3/min): (C) B = 500 dm^3/h, D = 2%; (D) B = 500 dm^3/h, D = 5%; (E) B = 700 dm^3/h, D = 5%.

Glass Transition Temperatures of Unprocessed and Spray-Dried UFH

DSC (10 K/min) of unprocessed UFH shows a broad endothermic event (100–180°C, Figure 4A), which is ascribed to the evaporation of the large amount of associated water. For each sample, HDSC (500 K/min) showed a baseline displacement, attributable to a glass transition (onset temperature T_g; Figure 4B–D). Values of T_g, respectively, for dried (115°C, 12 h) unprocessed, undried unprocessed, and spray-dried UFHs (Table 2) are close to those either in previous work or estimated using the Gordon-Taylor equation (Equation 1, Gordon & Taylor, 1952), in which the constant K was determined using the Simha-Boyer rule (Equation 2, Simha & Boyer, 1962):

$$T_{gmix} = \frac{(w_1 T_{g1}) + (K w_2 T_{g2})}{w_1 + (K w_2)} \quad (1)$$

$$K = \frac{\rho_1 T_{g1}}{\rho_2 T_{g2}} \quad (2)$$

($T_{g\,mix}$ is the glass transition onset temperature [absolute] for undried UFH. T_{g1}, T_{g2}; w_1, w_2 and ρ_1, ρ_2 are, respectively, the glass transition onset temperatures, mass fractions, and densities for water (1) and dry UFH (2). Values: T_{g1} = 130 K and T_{g2} = 444 K; ρ_1 = 1000 kg/m^3 and ρ_2 = 1900 kg/m^3; Hancock & Zografi, 1994.)

The closeness of observed and calculated values of T_g shows that plasticization of UFH by water is the most important factor influencing this transition.

The Plasticizing Effect of Water on Spray-Dried UFH

Using the DVS microbalance, spray-dried UFH was equilibrated at controlled RHs (30–90%), and Table 3 shows the corresponding values of the water content and T_g of the material. Even at low RH, spray-dried UFH sorbed considerable amounts of water, which lowered the T_g (e.g., by approximately ~120 K for 10%, wt/wt, of sorbed water). Above 47% RH, spray-dried UFH sorbed sufficient moisture to depress its T_g below 293 K. Agglomeration was observed for powders with glass transitions below ambient temperature. Therefore, for stability, spray-dried UFH should be stored under cool but dry conditions.

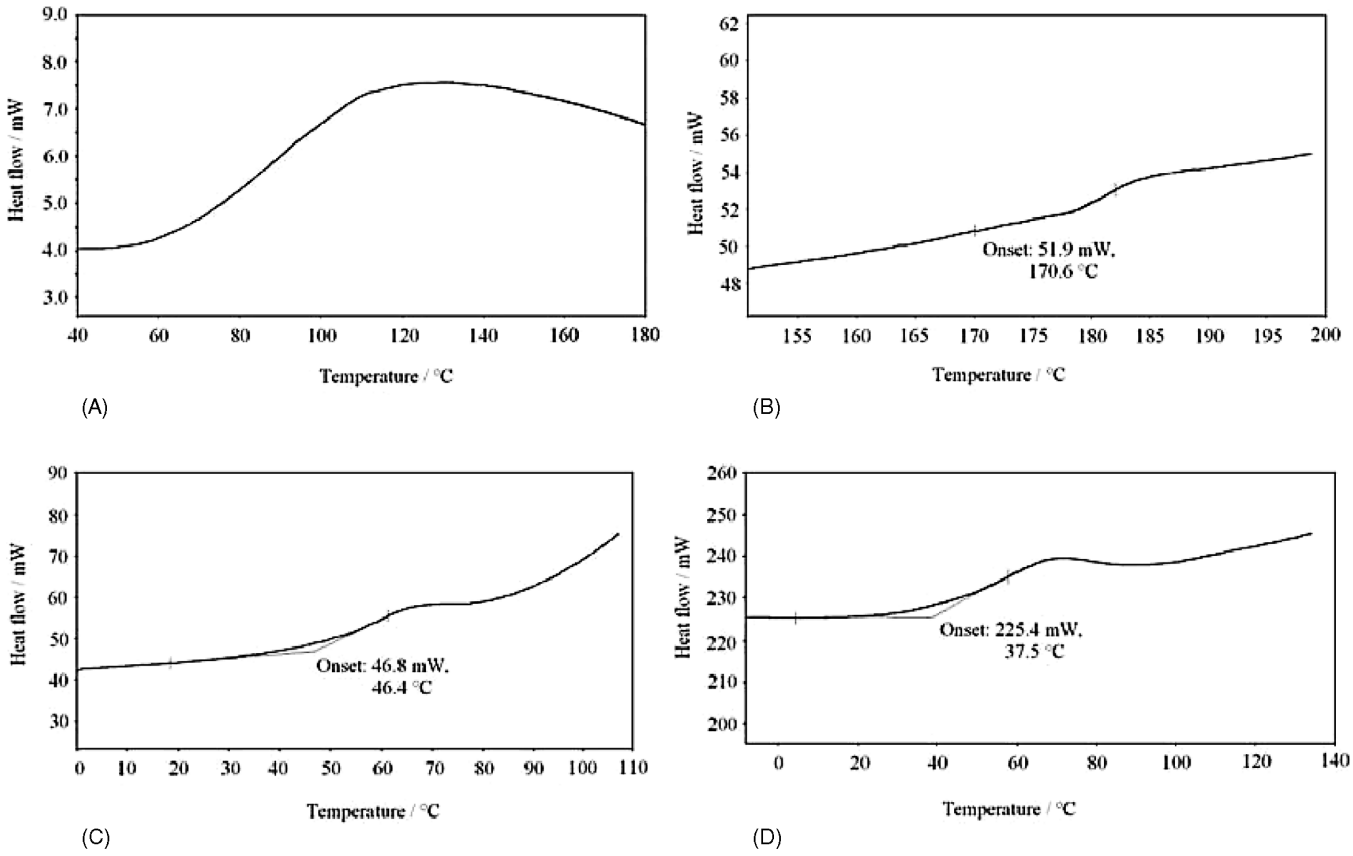

FIGURE 4. Differential scanning calorimetry (DSC) thermograms of (A) undried unprocessed unfractionated heparin (UFH) (10 K/min), (B) oven-dried unprocessed UFH (500 K/min), (C) undried unprocessed UFH (500 K/min), and (D) spray-dried UFH (500 K/min). Extrapolated onset glass-transition temperatures (T_g) are shown as the intersections of tangents.

TABLE 2
Glass Transition Onset Temperatures T_g for UFH

UFH	Moisture (%wt/wt)	T_g Observed (K)	T_g Calculated (K)
Dried unprocessed	(0)	444	—
Undried unprocessed	10.9	323	309
Spray-dried	11.5	311	304

UFH, unfractionated heparin.

TABLE 3
Absorption of Water (Fractional Change in Mass Δm) by Spray-Dried UFH in Moist Air (25°C) and Calculated Glass Transition Temperatures of the Hydrated Products

RH (%)	Δm (% wt/wt)	Mass Fraction of Water	T_g Calculated (K)
30.0	10.6	0.096	320
40.0	13.7	0.121	300
50.0	17.0	0.146	284
60.0	20.8	0.172	268
70.0	25.5	0.203	253
80.0	31.5	0.240	238
90.0	39.1	0.492	178

RH, relative humidity; UFH, unfractionated heparin.

Spray Drying of UFH

Production Characteristics, Operating Variables, and Parametric Analysis

A size distribution for spray-dried particles was obtained for each batch run in a series of 16 (conditions as per Table 1), carried out in random order (Table 4). All distributions showed features similar to those in Figure 5A. Individual distributions were characterized by the particle diameters $X_{n,}$ corresponding to cumulative percentages n = 50 and n = 90; approximately 95% of all product material was in the size range 0.5–10 μm. Small amounts of agglomerated material (10–15 μm) were detected.

Between the batches, there were considerable variations in the particle size distributions, with X_{50} values between 1.7 and 3.9 μm and X_{90} between 3.9 and 9.3 μm. Smaller particle sizes were favored by dilute feed solutions and high spray flow rates (Figure 4 and Table 4). To evaluate the dependence of the production characteristics (P representing percentage yield Y, the outlet temperature T_o, and the distribution characteristics X_{50} and X_{90}) on the four spray-drying variables A–D, the results were used to optimize (maximizing the correlation coefficient R^2) equations of the form

$$P = aA + bB + cC + dD + \sum_{\text{cross-terms}} n_{AB}AB$$

where a to d and all n are empirical coefficients.

Analysis of variance (ANOVA; Minitab, release 14, PA, USA) was used to plot Pareto charts (Figure 5B–E) to determine the variables and/or cross-terms that had a significant effect on the production characteristics at the 95% significance level (de Amorim, Bof, Franco, da Silva, & Nascentes, 2006; Garrido-López & Tena, 2005; Rezzoug & Capart, 2003).

The contributions of the significant variables, with coefficients, to each spray-drying characteristic are expressed in equations (Table 5). The high values of R^2 for these equations establish their reliability for the ranges of spray-drying conditions used, and only one cross-term is significant (X_{50}, Figure 5C).

Yield

The yield Y varied between 55 and 85% (Table 4), and was determined mainly by using the spray flow rate B and the feed solution concentration D (Figure 5B). The equation for Y (Table 5) shows that product yield is increased by increasing D and decreasing B, but is not affected by changing the pump speed A or inlet temperature C. Increasing B by 40% from 500 dm^3/h lowered the average Y from 75 to 65%. Decreasing D (5 to 2%, wt/vol) produced a similar decrease in Y. Both of these effects are attributed to a corresponding decrease in average particle size following the production of smaller atomized droplets due to, respectively, the increased atomization energy, and the decreased viscosity of the solution. The positive correlation between yield and particle size (Figure 6) shows that a greater proportion of smaller particles escapes capture by the cyclone, as the centrifugal forces are insufficient to drive these particles to the spray-dryer collector. Similar results were found by Millqvist-Fureby, Elofsson, and Bergenstahl (2001) for the spray drying of insulin, with no significant interaction between inlet air temperature and pump speed.

Particle Sizes

Mucopurulent plugging of the bronchi and bronchioles is universally present in CF patients from the age of 6 years, and in many younger patients (Bedrossian, Greenberg, Singer, Hansen, & Rosenberg, 1976). Targeting drugs to these areas depends on a number of factors, including particle size, breathing pattern, airway geometry, and hygroscopic growth of the particles as the RH increases from 0.5 in the upper airway to 0.995 within the lung (Heyder, 2004). Deposition patterns are affected by the reduced airway caliber in CF, which enhances

TABLE 4
Yields and Particle Size Distribution Characteristics, X_{50} and X_{90}, for the Randomized Sequence of Spray-Drying Runs in the Factorial Experiment

Run Order	Pump Speed (cm^3/min)	Spray Flow Rate (dm^3/h)	Inlet Temperature (°C)	UFH Concentration (% wt/vol)	Yield (%)	X_{50} (μm)	X_{90} (μm)	Outlet Temperature (°C)
1	8	500	160	2	65	2.6	6.6	90
2	8	500	180	5	82	3.7	8.7	96
3	8	700	160	2	65	1.7	3.9	72
4	5	700	160	2	55	1.8	3.9	95
5	5	500	160	2	60	2.6	6.3	91
6	8	700	180	5	66	2.4	5.8	92
7	5	700	160	5	66	2.4	5.4	93
8	5	700	180	2	65	1.8	4.1	105
9	8	500	180	2	80	2.5	6.1	99
10	8	700	180	2	55	1.8	4.0	102
11	5	500	180	2	65	2.3	5.6	108
12	5	500	160	5	80	3.3	7.7	75
13	8	700	160	5	84	2.4	5.7	85
14	8	500	160	5	86	3.9	9.3	85
15	5	700	180	5	66	2.3	5.3	103
16	5	500	180	5	82	3.5	8.3	101

UFH, unfractionated heparin.

delivery of drugs to the congested airways (Martonen et al., 1995), the site for mucolytic drug deposition. Targeting the small airways in CF may be achieved with particles of size 1–6 μm (Heyder, Laube, Jashnani, Dalby, & Zeitlin, 2000). We have investigated the spray-drying parameters required to achieve particles in this size range. However, the pulmonary deposition of inhaled heparin remains to be tested in vivo in CF patients. Particle size distributions (Figure 5A and Table 4), as characterized for each run by X_{50} (overall mean 2.5 μm, range 1.7–3.9 μm) and X_{90} (overall mean 6.0 μm, range 3.9–8.7 μm), were determined mainly by using the feed solution concentration D and the spray flow rate B, with a second-order term in these variables contributing significantly. X_{90} was also affected by the pumping speed A. Using the 2% (wt/vol) UFH solution gave reduced particle sizes (mean X_{50} = 2.1 μm, and X_{90} = 5.0 μm), whereas 5% (wt/vol) UFH gave larger particles (mean X_{50} = 3.0 μm and X_{90} = 7.0 μm). More concentrated (and hence more viscous) feed solutions will have produced coarser spray droplets and hence larger particles. High atomization energies are required to generate sprays of small droplets from such solutions. Correspondingly, the higher flow rate gave smaller particles (500 dm^3/h: X_{50} = 3.5 μm, X_{90} = 7.0 μm; 700 dm^3/h: X_{50} = 2.0 μm, X_{90} = 4.0 μm, respectively).

A significant second-order interaction between spray flow rate and feed concentration (BD) influenced the value of X_{50}, consistently with a proportion of the atomization energy being involved in working against viscous forces. A very large atomizing spray flow rate will be required to overcome the relative high viscosity of concentrated feed solutions, so as to nullify the effect of concentration on the particle size. Roos (1993) has reported that in the spray drying of dilute solutions of carbohydrates, highly soluble compounds (dextran, sucrose) form smaller particles than the less soluble lactose and mannitol. Therefore, 5% (wt/vol) aqueous UFH, being almost saturated, is likely to have formed the larger droplets that evaporate to larger particles. Dilute UFH solutions would be required for the production of small particles, but then aggregation would tend to occur.

The effect of pumping speed A on X_{50} was insignificant, but a small effect on X_{90} was identified (at A = 5 cm^3/min, X_{90} = 5.8 μm and at A = 8 cm^3/min, X_{90} = 6.2 μm). A lower pump speed tends to give both higher energy and more efficient atomization, although the effects are not large over the range of speeds used.

Outlet Temperature

The outlet temperature T_o is significant with regard to the thermal stability of materials being processed. Not unexpectedly, T_o (average increase from 86 to 101°C) responded strongly to the inlet temperature C (increased from 160 to 180°C; Table 4).

Optimization of Process Variables

With all the product characteristics being considered to be equally important, an optimization was performed (Minitab:

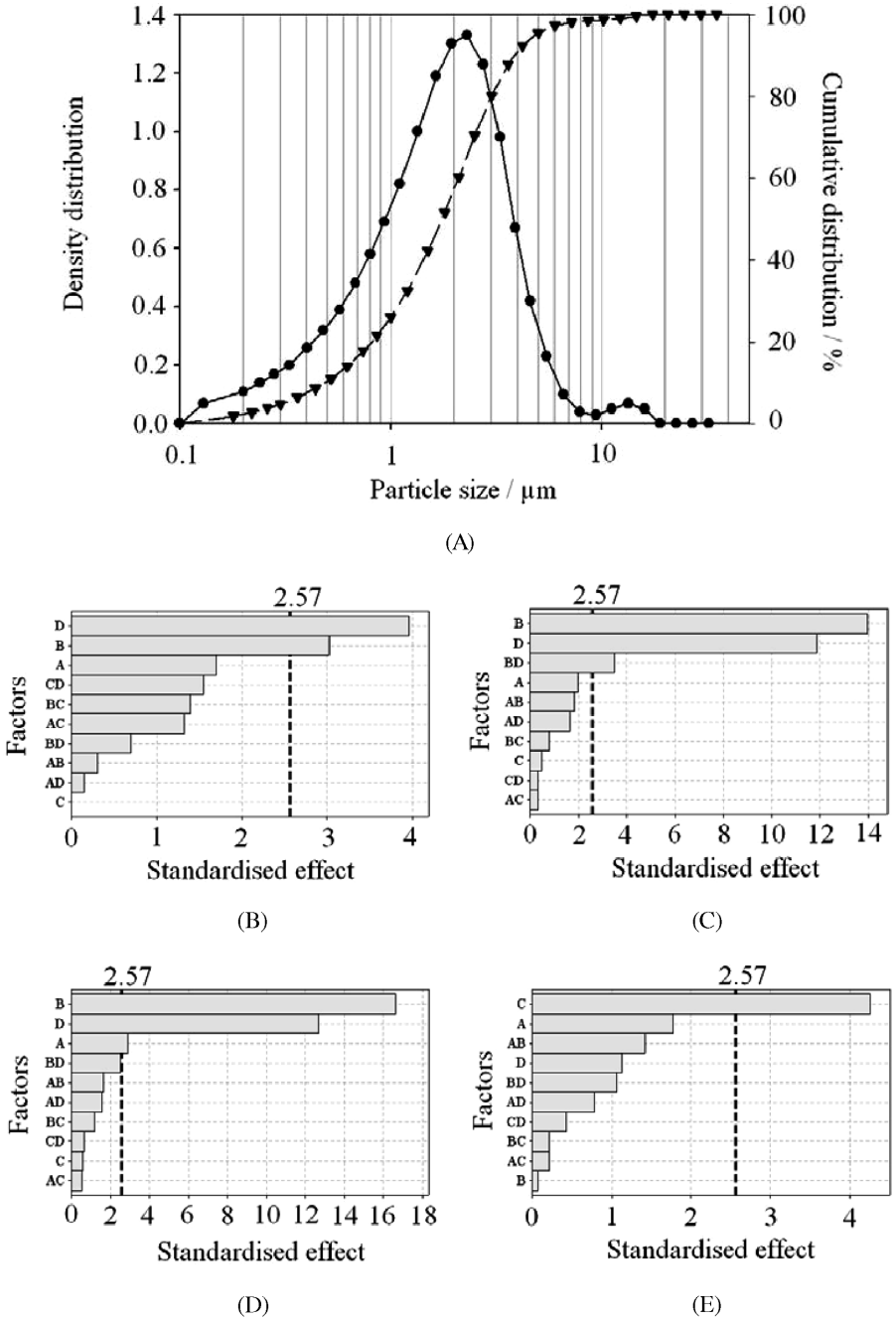

FIGURE 5. Particle size distribution of spray-dried unfractionated heparin (UFH): (A) density (●) and cumulative distributions (▼) for a batch run (Table 4, run 5). (B–E) Pareto charts of the product characteristics represented by the optimized values of the spray-drying process variables (pump speed *A* [cm^3/s], spray flow rate *B* [dm^3/h], inlet temperature *C* [°C], feed concentration *D* [% wt/vol]): (B) *Y*, (C) X_{50}, (D) X_{90}, and (E) T_o. (Bars extending beyond the 95% confidence interval (vertical line, 2.57) are significant.)

Response Optimization Function; Derringer & Suich, 1980) to find the individual desired value for each process variable, so as to maximize the yield and minimize the mean particle size of the product. The predicted optimal conditions were as follows: UFH concentration, 2%, wt/vol (aqueous); pneumatic nozzle, 7 mm; pump speed, 5 cm^3/min; spray flow rate, 700 dm^3/h; aspirator rate, 35 m^3/h; inlet temperature, 160–163°C; and outlet temperature, 90–95°C. Using these settings, a product with the following characteristics was predicted: $Y = 75 \pm 5\%$, $X_{50} = 2.3 \pm 0.4$ µm.

TABLE 5
Fitted Equations, Containing Terms Significant Above the 95% Confidence Level, for the Dependence of Product Characteristics (Yield Y, Distribution Characteristics X_{50}, X_{90}, and Outlet Temperature T_o) on Spray-Drying Process Variables (Pump Speed A [cm^3/s], Spray Flow Rate B [dm^3/h], Inlet Temperature C [°C], and Feed Concentration D [% wt/vol])

Fitted Equation	R^2 (%)
$Y = 70.1 - 4.88B + 6.38D$	94.9
$X_{50} = 2.56 - 0.494B + 0.419D - 0.123BD$	95.5
$X_{90} = 6.03 + 0.223A - 1.27B + 0.970D - 0.194BD$	97.3
$T_o = 93.3 + 7.50C$	95.7

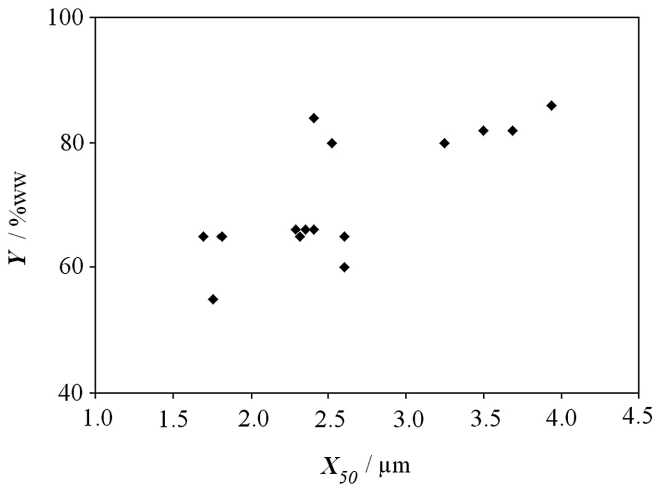

FIGURE 6. Corresponding values of the product yield Y and the particle size measure X_{50}, for all runs in the factorial experiment.

CONCLUSION

UFH has been spray-dried to produce particles in the inhalable size range (2–5 μm; recovery > 60%) that are potentially suitable for inhalation and deposition in peripheral and central airways. Of four process variables (feed concentration, atomization spray flow rate, inlet air temperature, and pump speed) evaluated by factorial experimental design, the first two had the greatest effects on the yield and the particle sizes of spray-dried UFH. To produce particles in the respirable range, UFH must be spray-dried from dilute solution and at a high atomization spray flow rate.

ACKNOWLEDGMENTS

We thank John Booth (Scientific and Medical Products Ltd, Cheadle, Manchester) for use of DVS equipment and Paul Gabbot and Paul Clarke (PETA Solutions, Oxford) for use of thermal analysis facilities. Jagdeep Shur is grateful to the Institute of Biomedical and Biomolecular Science (IBBS), University of Portsmouth, for providing a studentship.

NOMENCLATURE

Abbreviations

CF	Cystic fibrosis
CFTR	Cystic fibrosis transmembrane conductance regulator
DPI	Dry-powder inhaler
DSC	Differential scanning calorimetry
DVS	Dynamic vapor sorption
HDSC	Hyper differential scanning calorimetry
IR	Infrared
LMWH	Low-molecular-weight heparin
LRT	Lower respiratory tract
RH	Relative humidity
SEM	Scanning electron microscopy
TGA	Thermogravimetric analysis
UFH	Unfractionated heparin
XRPD	X-ray powder diffraction

Terms

A	Feed pump rate factor
B	Spray flow rate factor
C	Inlet temperature factor
D	Feed concentration factor
K	Constant
N	Number
P	Production characteristic
T_g	Glass transition onset temperature (K)
$T_{g\ mix}$	Glass transition onset temperature for undried UFH (K)
T_{g1}	Glass transition onset temperature for water (K)
T_{g2}	Glass transition onset temperature for dry UFH (K)
T_o	Outlet temperature (°C)
w_1	Mass fraction of water
w_2	Mass fraction of dry UFH
X_{10}	10% undersize particle size (μm)
X_{50}	50% undersize particle size (μm)
X_{90}	90% undersize particle size (μm)
Y	Yield (%)
ρ_1	Density of water (kg/m^3)
ρ_2	Density of dry UFH (kg/m^3)

REFERENCES

Balfour-Lynn, I. M., Klein, N. J., & Dinwiddie, R. (1997). Randomised controlled trial of inhaled corticosteroids (fluticasone propionate) in cystic fibrosis. *Arch. Dis. Child., 77*, 124–130.

Bedrossian, C. W. M., Greenberg, S. D., Singer, D. B., Hansen, J. J., & Rosenberg, H. S. (1976). The lung in cystic fibrosis. *Hum. Pathol., 7*, 195–204.

Bendstrup, K. E., Chambers, C. B., Jensen, J. I., & Newhouse, M. T. (1999a). Lung deposition and clearance of inhaled 99mTc-heparin in healthy volunteers. *Am. J. Respir. Crit. Care Med., 160*, 1653–1658.

Bendstrup, K. E., Gram, J., & Jensen, J. I. (2002). Effect of inhaled heparin on lung function and coagulation in healthy volunteers. *Eur. Respir. J., 19*, 606–610.

Bendstrup, K. E., Newhouse, M. T., Pedersen, O. F., & Jensen, J. I. (1999b). Characterisation of heparin aerosols generated in jet and ultrasonic nebulisers. *J. Aerosol Med., 12*, 17–25.

Blouquit, S., Regnier, A., Dannhoffer, L., Fermanian, C., Naline, E., Boucher, R., & Chinet, T. (2006). Ion and fluid transport properties of small airways in cystic fibrosis. *Am. J. Respir. Crit. Care Med., 174*, 299–305

Boucher, R. C. (2004). New concepts of the pathogenesis of cystic fibrosis lung disease. *Eur. Respir. J., 23*, 146–158.

Broadhead, J., Rouan, S. K. E., & Rhodes, C. T. (1992). The spray drying of pharmaceuticals. *Drug Dev. Ind. Pharm., 18*, 1169–1206.

Broughton-Head, V. J., Carroll, M. P., & Shute, J. K. (2005). Unfractionated heparin reduces the elasticity and yield stress of CF sputum. *J. Cyst. Fibros., 4*(S1), A102.

Broughton-Head, V. J., Smith, J. R., Shur, J., & Shute, J. K. (2006). Actin limits enhancement of nanoparticle diffusion through cystic fibrosis sputum by mucolytics. *Pulm. Pharmacol. Ther.*, doi:10.1016/j.pupt.2006.08.008.

Byron, P. R., & Patton, J. S. (1994). Drug delivery via the respiratory tract. *J. Aerosol Med. Deposition Clear. Eff. Lung, 7*, 49–75.

Coleman, D. E., & Montgomery, D. C. (1993). A systematic approach to planning for a designed industrial experiment. *Technometrics, 35*, 1–12.

Davis, P. B., Drumm, M., & Konstan, M. W. (1996). Cystic fibrosis. *Am. J. Respir. Crit. Care Med., 154*, 1229–1256.

de Amorim, F. V., Bof, C., Franco, M. B., da Silva, J. B. B., & Nascentes, C. C. (2006). Comparative study of conventional and multivariate methods for aluminium determination in soft drinks by graphite furnace atomic absorption spectroscopy. *Microchem. J., 82*, 168–173.

Derringer, G., & Suich, R. (1980). Simultaneous optimization of several response variables. *J. Qual. Technol., 12*, 214–219.

Fernández, C., Hattan, C. M., & Kerns, R. J. (2006). Semi-synthetic heparin derivatives: Chemical modifications of heparin beyond chain length, sulfate substitution pattern and N-sulfo/N-acetyl groups. *Carbohydr. Res., 341*, 1253–1265.

Frijlink, H. W., & de Boer, A. H. (2004). Dry powder inhalers for pulmonary drug delivery. *Exp. Opin. Drug Deliv., 1*, 67–86.

Garrido-López, A., & Tena, M. T. (2005). Experimental design approach for the optimisation of pressurised fluid extraction of additives from polyethylene films. *J. Chromatogr. A., 1099*, 75–83.

Geller, D. E. (2005). Comparing clinical features of the nebuliser, metereddose inhaler, and dry powder inhaler. *Respir. Care, 50*, 1313–1321.

Gordon, M., & Taylor, J. S. (1952). Ideal co-polymers and the second-order transitions of synthetic rubbers. 1. Non-crystalline co-polymers. *J. Appl. Chem., 2*, 493–500.

Haaland, P. D. (1989). *Experimental design in biotechnology*. New York: Marcel Dekker.

Hancock, B. C., & Zografi, G. (1994). The relationship between the glass-transition temperature and the water-content of amorphous pharmaceutical solids. *Pharm. Res., 11*, 471–477.

Heyder, J. (2004). Deposition of inhaled particles in the human respiratory tract and consequences for regional targeting in respiratory drug delivery. *Proc. Am. Thorac. Soc., 1*, 315–320.

Heyder, J., Laube, B. L., Jashnani, R., Dalby, R. N., & Zeitlin, P. L. (2000). Targeting aerosol deposition in patients with cystic fibrosis. Effects of alterations in particle size and inspiratory flow rate. *Chest, 118*, 1069–1076.

King, M., & Rubin, B. K. (2002). Pharmacological approaches to discovery and development of new mucolytic agents. *Adv. Drug Deliv. Rev., 54*, 1475–1490.

Kitson, C., Angel, B., Judd, D., Rothery, S., Severs, N. J., Dewar, A., Huang, L., Wadsworth, S. C., Cheng, S. H., Geddes, D. M., & Alton, E. W. F. W. (1999). The extra- and intracellular barriers to lipid and adenovirus-mediated pulmonary gene transfer in native sheep airway epithelium. *Gene Ther., 6*, 534–546.

Le Brun, P. P., de Boer, A. H., Heijerman, H. G., & Frijlink, H. W. (2000). A review of the technical aspects of drug nebulisation. *Pharm. World Sci., 22*, 75–81.

Ledson, M., Gallagher, M., Hart, C. A., & Walshaw, M. (2001). Nebulized heparin in Burkholderia cepacia colonized adult cystic fibrosis patients. *Eur. Respir. J., 17*, 36–38.

Lethem, M. I., James, S. L., Marriott, C., & Burke, J. F. (1990). The origin of DNA associated with mucus glycoproteins in cystic-fibrosis sputum. *Eur. Respir. J., 3*, 19–23.

Lewis, G. A., Mathieu, D., & Phan-Tan-Luu, R. (1999). *Pharmaceutical experimental design*. New York: Marcel Dekker.

Linsdell, P. (2006). Mechanism of chloride permeation in the cystic fibrosis transmembrane conductance regulator chloride channel. *Exp. Physiol., 91*, 123–129.

Martonen, T., Katz, I., & Cress, W. (1995). Aerosol deposition as a function of airway disease—cystic-fibrosis. *Pharm. Res., 12*, 96–102.

Masters, K. (1985). *Spray drying handbook* (4th ed.). New York: Longman Scientific & Technical and John Wiley and Sons.

Millqvist-Fureby, A., Elofsson, U., & Bergenstahl, B. (2001). Surface composition of spray-dried milk protein-stabilised emulsions in relation to pre-heat treatment of proteins. *Colloids Surf. B: Biointerfaces, 21*, 47–58.

Montgomery, D. C. (1997). *Design and analysis of experiments* (4th ed.). New York: John Wiley and Sons.

Perez-Vilar, J., & Boucher, R. C. (2004). Reevaluating gel-forming mucins' roles in cystic fibrosis lung disease. *Free Radic. Biol. Med., 37*, 1564–1577.

Rezzoug, S. A., & Capart, R. (2003). Assessment of wood liquefaction in acidified ethylene glycol using experimental design methodology. *Energy Convers. Manage., 44*, 781–792.

Riordan, J. R. (2005). Assembly of functional CFTR chloride channels. *Annu. Rev. Physiol., 67*, 701–718.

Roos, Y. H. (1993). Melting and glass transitions of low molecular weight carbohydrates. *Carbohydr. Res., 238*, 39–48.

Sanders, N. N., De Smedt, S. C., & Demeester, J. (2000). The physical properties of biogels and their permeability for macromolecular drugs and colloidal drug carriers. *J. Pharm. Sci., 89*, 835–849.

Serisier, D. J., Shute, J. K., Hockey, P. M., Higgins, B., Conway, J., & Carroll, M. P. (2006). Inhaled heparin in cystic fibrosis. *Eur. Respir. J., 27*, 354–358.

Simha, R., & Boyer, R. F. (1962). On a general relation involving the glass temperature and coefficients of expansion of polymers. *J. Chem. Phys., 37*, 1003–1007.

Taguchi, G. (1987). *System of experimental design*. New York: Unipub.

Tyrrell, D. J., Horne, A. P., Holme, K. R., Preuss, J. M., & Page, C. P. (1999). Heparin in inflammation: Potential therapeutic applications beyond anticoagulation. *Adv. Pharmacol., 46*, 151–208.

Vasconcellos, C., Drazen, J., Janmey, P. A., Wohl, M. E., Lind, S. E., & Stossel, T. P. (1993). Gelsolin reduces the viscosity of cystic-fibrosis sputum in vitro. *Clin. Res., 41*, A283.